

Defect evolution in ultrathin films of polystyrene-block-polymethylmethacrylate diblock copolymers observed by atomic force microscopy

J. Hahn,^{a)} W. A. Lopes,^{b)} H. M. Jaeger,^{b)} and S. J. Sibener^{a)}

The James Franck Institute, The University of Chicago, 5640 South Ellis Avenue, Chicago, Illinois 60637

(Received 11 August 1998; accepted 7 October 1998)

We track individual defects in the microdomain patterns of cylinder-forming polystyrene-block-polymethylmethacrylate films with atomic force microscopy to elucidate the evolution of diblock domain topology during annealing. This evolution takes place through relinking, joining, clustering, and annihilation of defects. Such processes form the basis for predicting structural change in polymer films. © 1998 American Institute of Physics. [S0021-9606(98)71047-5]

Diblock copolymer systems^{1,2} have drawn considerable attention in recent years due to both their technological promise for creating small devices^{3,4} as well as their rich phase behavior and associated complex kinetic processes which lead to the growth of order.⁵⁻⁷ The two chemically distinct, and thus immiscible, polymer blocks in diblock copolymers undergo phase separation and self-assemble into ordered patterns of microdomains whose characteristic size is determined by the polymer chain lengths. Defects in the local microdomain ordering play a crucial role in limiting the mechanical and dielectric properties of the material. Under the influence of thermal energy or applied external forces such as shear⁸ or electric field,⁹ the cooperative motion of individual polymer chains allows defects to propagate. To understand and control microdomain ordering it is therefore important to have an understanding of both the type of defects that might occur and their evolution over time. To this extent, the tracking of individual defects is highly desirable, but so far has been unobtainable. Here we report the first investigation of defect evolution in thin films of diblock copolymers by atomic force microscopy in which we have non-destructively imaged large sets of individual defects between repeated annealing cycles.

In bulk diblock copolymers microdomain ordering has previously been investigated by a variety of techniques, including optical birefringence,¹⁰⁻¹² neutron scattering,¹³ and small angle x-ray scattering (SAXS).¹⁴ Such scattering probes look at spatially averaged behavior and, consequently, cannot provide information about individual defects. Transmission electron microscopy (TEM)^{10,11} or scanning electron microscopy (SEM)¹⁵ can image individual defects, but typically have been applied to microtomed slices of bulk samples. The need to stain one of the copolymer domains for TEM or SEM contrast enhancement, as well as the irradiation damage by electron beams, however, mitigates the observation of the time evolution of individual defects. These difficulties are overcome by the use of atomic force microscopy (AFM). Unlike other techniques used to directly image

microdomains in copolymers, AFM has demonstrated a superb, nondestructive imaging capability. Thus, without affecting the evolution of the film, we can image a sample, anneal the sample so that it evolves further, quench the sample back to room temperature, and take another image of the *same film area*.

AFM imaging of the film surface faithfully represents the underlying microdomain morphology in polystyrene-block-polymethylmethacrylate (PS-b-PMMA) ultrathin films, as we have demonstrated previously.¹⁶ In that work, we showed through a direct comparison of AFM and (subsequent) TEM images of the *same* microdomains that the surface corrugation measured by the AFM is a few nm higher above the PMMA domains than over the PS domains. By imaging the evolution of the corrugation (and its associated defects) it is thus possible to noninvasively study the motion and evolution of individual defects. Using this technique we delineate different types of defects and monitor their evolution in single repeat spacing thick PS-b-PMMA films, and suggest possible mechanisms for the observed topological evolution.

The cylinder-forming diblock copolymer used in this study consisted of 74% PS by weight, had a molecular weight of 84 000 g/mol, and a polydispersity of 1.08. The repeat spacing of the single layer of cylinders aligned parallel to the film plane, as measured by AFM and TEM, was 50 nm. PS-b-PMMA ultrathin films (50 nm thick as measured by ellipsometry) were prepared by spin-coating onto silicon nitride substrates¹⁶ and annealed under an argon atmosphere. At elevated temperatures the wetting behavior of PS-b-PMMA coated onto a silicon nitride substrate is known; for this system the block with the lower wetting energy, PMMA, covers the substrate.¹⁶ Since polymer chains in the film become increasingly mobile above the material's glass temperature (approximately 375 K for our samples), the annealing temperature, annealing time, as well as the rate at which the samples are ramped down from the annealing temperature may affect the number and types of defects in the film.^{10,11} The experiments described in this paper were done under the following conditions: annealing temperature 523 K, annealing time 1 h, and ramp rates of 5 K/min from room

^{a)}Also at Department of Chemistry.

^{b)}Also at Department of Physics.

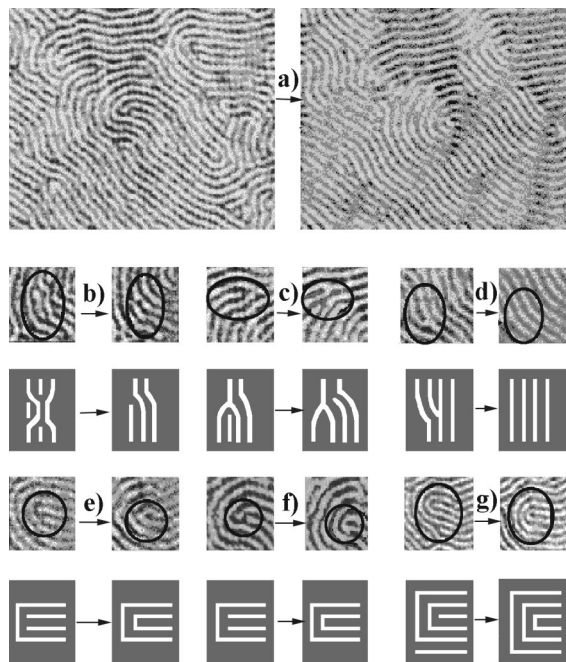


FIG. 1. Defect evolution by relinking and joining. Bright domains are PMMA, dark domains are PS. (a) $2 \mu\text{m}$ by $1.5 \mu\text{m}$ AFM images of microdomains annealed for 2 h (the left-hand side) and 3 h (the right-hand side) at 523 K. (b)–(f) $0.5 \mu\text{m}$ by $0.5 \mu\text{m}$ AFM images and associated schematics of defect change. Open-ended defects forming a Y joint (b) and (c), Y-joint annihilation (d), and two single-ended defects joining each other (e) and (f). (g) $1 \mu\text{m}$ by $1 \mu\text{m}$ AFM image and associated schematic showing defect evolution via relinking.

temperature to the annealing temperature and 2 K/min on cooling back down. The annealing temperature was carefully chosen: Samples annealed at temperatures below 510 K exhibited no noticeable changes in their microstructure for any duration of annealing. At about 515 K, using different annealing times of up to 60 h, the only noticeable changes were in domains having high curvature. Annealing at 523 K for 1 h was found to lead to noticeable defect evolution, i.e., local topological change, while preserving facile identification of the same region between annealing cycles. AFM imaging was performed with a Topometrix Discoverer, using a silicon nitride tip in contact mode and an applied force of 1 nN.

Figures 1 and 2 each present a set of consecutive AFM images, with the first image in each figure being taken following an initial 2 h annealing treatment; the second image in each figure was taken after the sample was subsequently subjected to a second 1 h annealing cycle. Figures 1(a) and 2(a) each show representative large-scale views of the domain structure in the films. The other panels of Figs. 1 and 2 show enlarged details of the Figs. 1(a) and 2(a) images. As a guide to the eye, we have included schematic representations of the domain structure in the detailed views. In all images, the light-colored regions correspond to corrugation maxima and thus PMMA microdomains.¹⁶ Observed over sufficiently large areas ($2 \mu\text{m} \times 2 \mu\text{m}$ or larger), the average defect density did not vary with the size of the chosen area. However, we found that the defect density decreases by 20% during the second anneal.

We now describe individual defects and their evolution

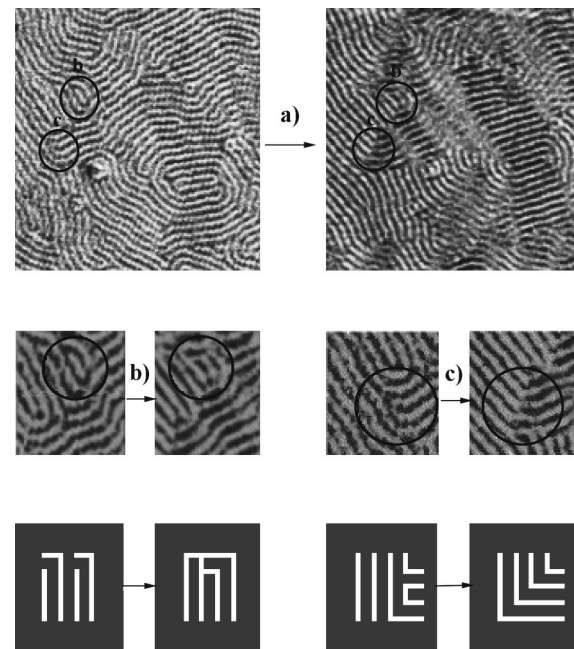


FIG. 2. Defect evolution via relinking and joining. Bright domains are PMMA, dark domains are PS. (a) $1.5 \mu\text{m}$ by $1.5 \mu\text{m}$ AFM images of microdomains annealed for 2 h (the left-hand side) and 3 h (the right-hand side) at 523 K. (b) and (c) $0.5 \mu\text{m}$ by $0.5 \mu\text{m}$ AFM images and associated schematics of defect change. Open ended defects forming a Y joint (b) and defect annihilation by relinking (c).

in more detail. We define a Y joint to be any place in the film where three microdomains join at a node. An initial defect consisting of a PMMA microdomain with open ends on both sides can connect one or both ends with one of the neighboring microdomains, making a temporary Y joint as shown in Figs. 1(c) and 2(b). Although the local structural environment is of obvious importance in guiding local topological change, these are common occurrences, with many instances of open ends after the first anneal evolving into Y joints during the second anneal. After a Y joint has been formed in this way, one of its branches becomes an open-ended defect which can then propagate through microdomains until it encounters and annihilates another defect. If two single open-ended defects are one repeat spacing apart, they can simply connect themselves, i.e., join, as shown in Figs. 1(e) and 1(f). For defects further apart, and noncollinear, a polymer domain next to a defect can reconfigure its geometrical arrangement via relinking, Figs. 1(g) and 2(c). The new defect line generated by this process propagates until it meets another defect. Figures 1 and 2 show evidence for joining, relinking, and annihilating simultaneously occurring at different places of the sample.

Defects can interact with other defects and propagate as a consequence of the stress fields they produce around their core.¹⁷ Much of the corresponding theory has been worked out and extensive observations are available from a variety of related systems, including liquid crystals (for a detailed discussion of this issue see, e.g., Ref. 11). While there are differences between a smectic liquid crystal system and a copolymer thin film, certain key aspects of the underlying physics carry over. Of particular interest is the fact that the

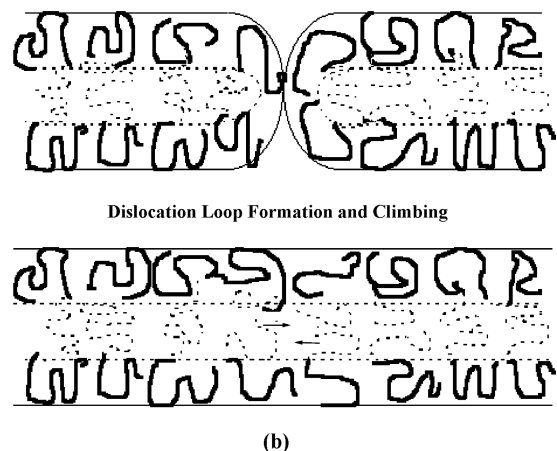
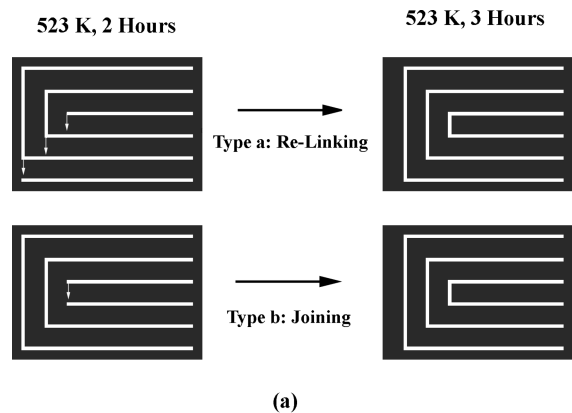


FIG. 3. Simplified model for defect change: combinations of gliding and climbing. (a) Proposed models for relinking and joining of polymer chains based on AFM images. (b) Defect annihilation at the molecular scale: forming a dislocation loop and climbing. Dashed and bold lines represent PMMA and PS, respectively.

interaction energy of two opposing, open-ended defects in liquid crystals is greatest when their regions of maximum strain overlap.¹⁷ These regions extend out from the defect core in a parabolic fashion, perpendicular to the plane of the liquid crystal. The topological structure for the microdomains of cylinder-forming PS-*b*-PMMA can be most closely identified with that of a columnar liquid crystal. However, many defect interaction studies have been performed on smectic liquid crystal systems (e.g., Ref. 17). Insights from these studies on smectic systems suggest for the microdomains in our thin films that two open-ended defects should have a longer interaction range when they are non-collinear. Indeed, within our annealing time and temperature window, we did not observe any direct interaction and annihilation events of collinear defects. On the other hand, we found many instances where noncollinear open-ended defects interacted over length scales as long as a few times the repeat spacing.

All defect motion we were able to image involved relinking and joining events as shown schematically in Fig. 3. Presumably, the underlying mechanism is due to dislocation loop formation and climbing,¹¹ Fig. 3. Even in a situation where direct interaction of wall defects might eventually proceed on a longer time scale, or under the influence of an electric field, over the 1 h annealing time in our experiments

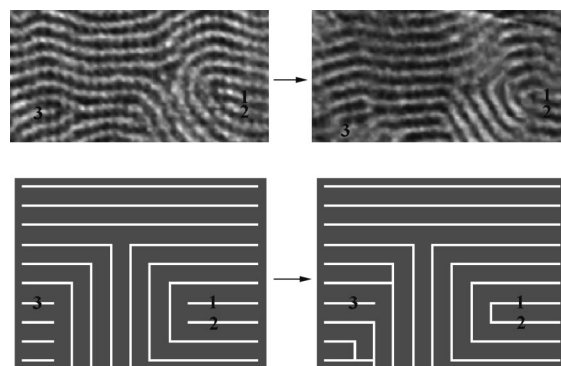


FIG. 4. Indirect interactions of defects: 1.2 μm by 0.6 μm AFM images and associated schematics of defect change annealed for 2 h (the left-hand side) and 3 h (the right-hand side) at 523 K. Defect 1 interacts indirectly with defect 2 rather than direct penetration through wall defects to join with defect 3.

we found indirect interaction of line defects to dominate. This is shown in Fig. 4 where, rather than observing direct interaction of two wall defects, we find several relinking and joining events of line defects on either side of the walls.

Given the hierarchy of defect stability and evolution pathways reported in this communication, we can now begin to propose likely scenarios for defect change during annealing. Such understanding is an essential prerequisite for being able to predict the thermally activated structural changes that occur within thin polymer films. Figure 5(a) shows a series of such predictions. In the first panel of Fig. 5(a), PS microdomains (dark domains) contain two Y-joint defects, one single-ended defect, and one double-ended defect. Annealing would be expected to modify the structure of these domains by either reducing the total number of defects or by changing the defect configuration into a more stable form. In the last

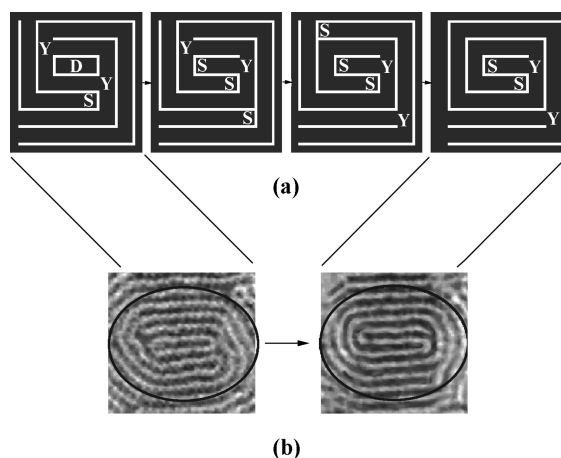


FIG. 5. Predicted scenario and associated experimental evidence for defect evolution. Bright domains are PMMA and dark domains are PS. (a) Schematic representation of likely scenario for defect evolution. Types and numbers of PS defects are: (1) two Y joints, one single ended, and one double ended; (2) and (3) two Y joints and three single ended; (4) two Y joints and two single ended. The letter Y denotes a Y joint, S denotes a single-ended defect, and D denotes a double-ended defect. (b) Experimental images following the predicted behavior: 0.75 μm by 0.75 μm AFM images of a sample annealed for 2 h (the left-hand side) and for 3 h (the right-hand side) at 523 K.

panel of Fig. 5(a), PS microdomains have evolved into two Y-joint defects and two single-ended defects. Figure 5(b) displays a sequence of actual AFM images taken before and after an annealing cycle which matches the predictions of Fig. 5(a).

In conclusion, we have performed the first direct tracking experiments of how individual defects evolve in diblock copolymer films between repeated cycles of annealing. This was accomplished using atomic force microscopy to image the surface corrugation of ultrathin asymmetric PS-*b*-PMMA films, films which contained a single layer of PMMA cylinders oriented parallel to the film plane. The evolution of defects with a Y joint, two open ends, and one open end were monitored. Over the experimental parameter window (523 K annealing temperature, 1 h annealing time) we found Y joints to be the most stable defect configuration, followed by single-ended and then double-ended defect domains. Our results give direct evidence for defect evolution based on mechanisms such as relinking, joining, clustering, and annihilation of defects. This work is now being extended to encompass kinetic measurements of domain evolution as a function of annealing conditions. Our hope is that the combined understanding of topological changes, such as those reported in this paper, when combined with mobility kinetics, will give us a predictive understanding of the thermally activated structural changes that occur within thin polymer films.

It is with pleasure that we thank Tom Witten for valuable discussions. This work was supported by the MRSEC

program of the National Science Foundation at The University of Chicago, Award No. DMR-9808595, and, in part, by the Air Force Office of Scientific Research (AFOSR and DoD-URI).

- ¹F. S. Bates and G. H. Fredrickson, *Annu. Rev. Phys. Chem.* **41**, 525 (1991).
- ²G. H. Fredrickson and F. S. Bates, *Annu. Rev. Mater. Sci.* **26**, 501 (1996).
- ³R. W. Zehner, W. A. Lopes, T. L. Morkved, H. M. Jaeger, and L. R. Sita, *Langmuir* **14**, 241 (1998).
- ⁴M. Park, C. Harrison, P. Mansky, and P. M. Chaikin, *Science* **276**, 1401 (1997).
- ⁵H. J. Dai, N. P. Balsara, B. A. Garetz, and M. C. Newstein, *Phys. Rev. Lett.* **77**, 3677 (1996).
- ⁶Y. Shiwa, T. Taneike, and Y. Yokojima, *Phys. Rev. Lett.* **77**, 4378 (1996).
- ⁷C. Harrison, M. Park, P. M. Chaikin, R. A. Register, and D. H. Adamson, *J. Vac. Sci. Technol. B* **16**, 544 (1998).
- ⁸Z. R. Chen and J. A. Kornfield, *Polymer* **39**, 4679 (1998).
- ⁹T. Morkved, M. Lu, A. M. Urbas, E. E. Ehrichs, and H. M. Jaeger, *Science* **273**, 931 (1996).
- ¹⁰K. Amundson, E. Helfand, X. Quan, and S. D. Smith, *Macromolecules* **26**, 2698 (1993).
- ¹¹K. Amundson, E. Helfand, X. Quan, and S. D. Smith, *Macromolecules* **27**, 6559 (1994).
- ¹²K. Amundson, E. Helfand, S. S. Patel, X. Quan, and S. D. Smith, *Macromolecules* **25**, 1935 (1992).
- ¹³A. Karim, N. Singh, M. Sikka, F. S. Bates, W. D. Dozier, and G. P. Flecher, *J. Chem. Phys.* **100**, 1620 (1994).
- ¹⁴K. Amundson, E. Helfand, D. D. Davis, X. Quan, S. S. Patel, and S. D. Smith, *Macromolecules* **24**, 6546 (1991).
- ¹⁵C. Harrison, M. Park, P. M. Chaikin, R. A. Register, D. H. Adamson, and N. Yao, *Polymer* **39**, 2733 (1998).
- ¹⁶T. Morkved, W. A. Lopes, J. Hahm, S. J. Sibener, and H. M. Jaeger, *Polymer* **39**, 3871 (1998).
- ¹⁷P. M. Chaikin and T. C. Lubensky, *Principles of Condensed Matter Physics* (Cambridge University Press, Cambridge, 1995), Chap. 9.